Biogeosciences, 11, 2755–2770, 2014
www.biogeosciences.net/11/2755/2014/
doi:10.5194/bg-11-2755-2014

Ocean–atmosphere exchange of organic carbon and CO_2 surrounding the Antarctic Peninsula

S. Ruiz-Halpern[1,7], M. Ll. Calleja[2], J. Dachs[3], S. Del Vento[3,4], M. Pastor[5], M. Palmer[1], S. Agustí[1,6], and C. M. Duarte[1,6]

[1]Instituto Mediterráneo de Estudios Avanzados (IMEDEA), Consejo Superior de Investigaciones Científicas-Universitat de les Illes Balears (CSIC-UIB), Esporles, I. Balears, Spain
[2]Instituto Andaluz de Ciencias de la Tierra (IACT), Consejo Superior de Investigaciones Científicas – Universidad de Granada (CSIC-UGR), Avda. de las Palmeras 4, 18100 Armilla, Granada, Andalusia, Spain
[3]Department of Environmental Chemistry, Institute of Environmental Assessment and Water Research (IDAEA), Consejo Superior de Investigaciones Científicas (CSIC), Barcelona, Catalonia, Spain
[4]Lancaster Environment Centre, Lancaster University, Lancaster LA1 4YQ, UK
[5]Departamento de Acústica y Geofísica Unidad de Tecnología Marina-Consejo Superior de Investigaciones Científicas (UTM-CSIC), Barcelona, Catalonia, Spain
[6]The UWA Oceans Institute and School of Plant Biology, University of Western Australia, 35 Stirling Highway, Crawley 6009, Australia
[7]Centre for Coastal Biogeochemistry, School of Environment, Science and Engineering, Southern Cross University, Lismore, New South Wales, Australia

Correspondence to: S. Ruiz-Halpern (sergio.ruiz-halpern@scu.edu.au)

Received: 28 August 2013 – Published in Biogeosciences Discuss.: 21 October 2013
Revised: 2 April 2014 – Accepted: 11 April 2014 – Published: 26 May 2014

Abstract. Exchangeable organic carbon (OC) dynamics and CO_2 fluxes in the Antarctic Peninsula during austral summer were highly variable, but the region appeared to be a net sink for OC and nearly in balance for CO_2. Surface exchangeable dissolved organic carbon (EDOC) measurements had a 43 ± 3 (standard error, hereafter SE) $\mu mol\,C\,L^{-1}$ overall mean and represented around 66 % of surface non-purgeable dissolved organic carbon (DOC) in Antarctic waters, while the mean concentration of the gaseous fraction of organic carbon (GOC H'^{-1}) was 46 ± 3 SE $\mu mol\,C\,L^{-1}$. There was a tendency towards low fugacity of dissolved CO_2 (fCO_{2-w}) in waters with high chlorophyll *a* (Chl *a*) content and high fCO_{2-w} in areas with high krill densities. However, such relationships were not found for EDOC. The depth profiles of EDOC were also quite variable and occasionally followed Chl *a* profiles. The diel cycles of EDOC showed two distinct peaks, in the middle of the day and the middle of the short austral dark period, concurrent with solar radiation maxima and krill night migration patterns. However, no evident diel pattern for GOC H'^{-1} or CO_2 was observed. The pool of exchangeable OC is an important and active compartment of the carbon budget surrounding the Antarctic Peninsula and adds to previous studies highlighting its importance in the redistribution of carbon in marine environments.

1 Introduction

The ocean and the atmosphere exchange momentum, heat, gas and materials across an area of $361 \times 10^6\,km^2$. These interactions play a major role in the dynamics of the Earth's system (Siedler et al., 2001). Gas exchange plays a key role in climate regulation, as oceans have already absorbed a large fraction of anthropogenically produced CO_2 (Sabine et al., 2004), the major greenhouse gas (GHG) contributing to global warming. However, vast heterotrophic areas are found in the open ocean (which release CO_2), fueled by allochthonous DOC inputs (Del Giorgio and Duarte, 2002), and the metabolic status of the ocean still remains under debate (Ducklow and Doney, 2013, and references therein).

Furthermore, the ocean can also be a source of other climatically active gases, such as methane (Judd et al., 2002) and dimethyl sulfide (DMS) (Charlson et al., 1987; Ayers and Gillett, 2000), and there is an active exchange of volatile and semivolatile organic compounds (VOCs and SOCs) across the air–sea boundary (where they can be remineralized or exported downwards). However, a comprehensive assessment of the magnitude of these fluxes is still lacking.

Although there have been some attempts to summarize gas-phase organic carbon compounds (Heald et al., 2008), Goldstein and Galbally (2007) predict that over a million types of C_{10} compounds (molecules with 10 carbon atoms) are likely to exist in the atmosphere, precluding the resolution of organic carbon fluxes between the ocean and the atmosphere on a single-compound basis. Hence, the focus on a few relevant volatile and semi-volatile organic compounds, usually measured in marine ecosystems (Laturnus, 2001; Sinha et al., 2007; Yang et al., 2013), which account for a small fraction of the VOC and SOC pool, do not allow for a quantitative estimation of the air–sea exchange of organic carbon at the ocean–atmosphere interphase. Furthermore, numerous reports in the literature demonstrate the production of single compounds or, at best, a modest set of individual VOCs and SOCs by marine organisms, from macroalgae to phytoplankton (Laturnus et al., 2000; Bravo-Linares et al., 2007), as well as remineralization by bacteria (Cleveland and Yavitt, 1998). These studies show that the production and consumption of exchangeable organic carbon is ubiquitous in the ocean (Giese et al., 1999). A large fraction of VOCs and SOCs are of anthropogenic origin and are also found in the atmosphere worldwide. Their exchange across the air–sea boundary is dominated by the diffusive fluxes from the gas phase to the dissolved phase, especially in the case of semi-volatile compounds (Hauser et al., 2013). However, there is no inventory of all anthropogenic SOCs over either the oceanic or terrestrial atmospheres. Thus, the quantification of the total amount of VOC and SOC exchanged between the oceans and the atmosphere remains challenging.

The problem is comparable to the attempt at estimating the pool of DOC in the ocean from the sum of the concentrations of the individual compounds. The solution adopted was the formulation of an operational definition of the DOC concept (Hansell and Carlson, 2002) that allows for the collective estimation of the total pool of compounds contributing to DOC in a single analysis (Spyres et al., 2000). Likewise, a pathway towards the estimation of the air–sea exchange of VOC and SOC is the formulation of an operational definition. Dachs et al. (2005) proposed collectively measuring VOC and SOC compounds as exchangeable dissolved organic carbon (EDOC), if measured in the water, or gaseous organic carbon (GOC H'^{-1}), if measured in equilibrium with the atmosphere (Dachs et al., 2005; Ruiz-Halpern et al., 2010). The concepts of EDOC and GOC H'^{-1} provide an approach comparable to that of conventional dissolved organic carbon (DOC) analysis to operationally quantify these compounds (in $\mu mol\,C\,L^{-1}$) beyond the limitations associated with approaches based on individual compounds, which have not been resolved for the marine DOC pool either.

EDOC and GOC H'^{-1} are exchanged dynamically across the air–sea boundary, a process that has been largely overlooked as it is currently missing from oceanic carbon budget assessments (Solomon et al., 2007). However, the few available studies have identified air–sea exchange of organic carbon as an important component of the carbon budget in the subtropical NE Atlantic (Dachs et al., 2005) and subarctic fjords (Ruiz-Halpern et al., 2010). These recently quantified fluxes are comparable in magnitude to the fluxes of CO_2 and organic aerosols combined (Jurado et al., 2008). Moreover, resolving EDOC is important because it is a component of DOC that is mostly not captured with conventional measurements of DOC (Spyres et al. 2000), as they only measure the non-purgeable organic carbon fraction, so the oceanic pool of total DOC is underestimated (Dachs et al., 2005).

Polar ecosystems are characterized by intense biological activity (Clarke et al., 1996). Thus, fluxes of exchangeable organic carbon are likely to be of regional or even global relevance. Ruiz-Halpern et al. (2010) identified cold marine environments as areas potentially supporting large air–sea organic carbon (OC) fluxes for a variety of reasons: (1) the Henry's law constant (H') is low at low temperatures, displacing exchangeable OC towards the water phase (Staudinger and Roberts, 2001); (2) polar macroalgae (Laturnus, 2001) and phytoplankton (Sinha et al., 2007) have already been identified as an important source of a wide variety of VOCs, including halogenated VOCs, acetone, acetaldehyde, DMS and isoprene; and (3) the increase in ice coverage in winter reduces the available area of air–sea OC exchanges, reducing their fluxes in winter and leading to a potential large release during summer ice melt (Ruiz-Halpern et al., 2010). Additionally, UV radiation, particularly high in the Antarctic spring and summer seasons (Madronich et al., 1998), may affect the stocks of exchangeable organic carbon in the water column by triggering phytoplankton cell death and lysis and the subsequent release of OC to the environment (Llabrés and Agustí, 2010), as well as through photochemical degradation of organic molecules, both in the water and the atmosphere (Zepp et al., 1998).

The Southern Ocean is particularly important in the regulation of the Earth's climate, as it is considered a sink for CO_2 (Sabine et al., 2004; Gruber et al., 2009) and connects the Pacific, Atlantic and Indian oceans. Understanding the carbon budget in the Southern Ocean is therefore of particular interest. Gas exchanges across the air–sea interface are controlled by temperature and wind speed, dependent upon the meteorological conditions, and influencing the air–water mass transfer coefficients. In addition, air–water fluxes also depend on the concentration gradient, which is controlled by rising concentrations in the atmosphere and the balance between sources and sinks in the water, including the surface microlayer, which can have a significant impact on air–sea exchange, even at moderate to high wind speeds (Liss and Duce, 2005), and are also a result of deposition processes in the atmosphere and biological activity in the ocean (Cunliffe et al., 2013). These processes are currently subjected to anthropogenic forcings due to rapid global change, including pollution, increasing atmospheric CO_2 concentrations and ocean acidification, as well as rising temperatures and wind speeds (Hardy, 1982; Young et al., 2011; Doney et al., 2009).

Unfortunately, whereas the air–sea fluxes of CO_2 have been evaluated extensively, there are no reported estimations of the air–sea fluxes of OC in the Southern Ocean. Here, we examine the pools of EDOC and GOC H'^{-1} and the associated air–sea exchanges of OC in the Antarctic Peninsula region, and compare these exchanges to the corresponding air–sea fluxes of CO_2. We estimate these parameters for the austral summers of years 2005, 2008 and 2009 from measurements taken during three cruises conducted along the Antarctic Peninsula onboard R/V *Hespérides*.

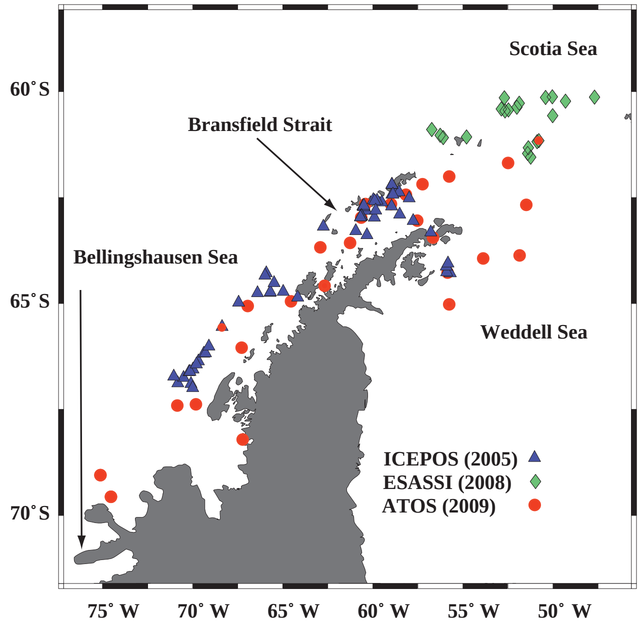

Figure 1. Map of the region and the stations sampled during the three cruises: ICEPOS 2005 (blue triangles), ESASSI 2008 (green diamonds) and ATOS-Antarctica 2009 (red circles).

2 Data set and methodology

2.1 Study site

Three cruises were conducted onboard the Spanish R/V *Hespérides* along the Antarctic Peninsula: ICEPOS (2 to 22 February 2005), ESASSI (5 to 16 January 2008) and ATOS-Antarctica (28 January to 23 February 2009). The ICEPOS and ATOS-Antarctica cruises followed similar trajectories around the Antarctic Peninsula. They covered the tip of the Antarctic Peninsula, from the Weddell Sea to Bransfield Strait, and its western coast. The ESASSI cruise was restricted to the northern edge of the Weddell Sea, between the South Shetland and South Orkney islands (Fig. 1).

2.2 Sampling

During the ICEPOS cruise, coupled measurements of EDOC in surface waters and GOC H'^{-1} were taken at 61 locations, whereas only 20 and 25 coupled measurements were taken during the ESASSI and ATOS-Antarctica cruises, respectively. Depth profiles of EDOC concentration in the water column were also performed during the ICEPOS and ATOS-Antarctica cruises. Additionally, several diel cycles and EDOC sampled at the surface microlayer (SML) were conducted during the ICEPOS cruise. Finally, concurrent measurements in air and water of CO_2 were taken along the cruise track.

2.3 CO_2 measurements

The mole fraction of CO_2 in air ($x\mathrm{CO}_{2-\mathrm{a}}$) was measured continuously at 1 min intervals with a commercially available high-precision (± 1 ppm) non-dispersive infrared gas analyzer (EGM4, PP systems), passing clean air that is free of emissions from the vessel through an anhydrous calcium sulfate (Drierite) column to remove water vapor and avoid interferences in the detector. Surface seawater molar fraction of CO_2 ($x\mathrm{CO}_{2-\mathrm{w}}$) was also measured at 1 min intervals and concurrently with atmospheric measurements by circulating water from a depth of 5 m, where the intake of the continuous flow-through system of the vessel is located. Water was pumped through a gas exchange column (1.25×9 membrane contactor, Celgard) and a closed-loop gas circuit fitted with an anhydrous calcium sulfate column, where CO_2 equilibrates, and is then circulated through the gas analyzer in the same manner as for the air measurements. The continuous flow of water and the small volume of air circulating counter-current through the gas exchange column ensured full and rapid equilibration between water and air (Calleja et al., 2005). The CO_2 measured in air and water corresponds to that in dry air ($x\mathrm{CO}_2$). Thus, fugacity of CO_2 in air ($f\mathrm{CO}_{2-\mathrm{a}}$) and water ($f\mathrm{CO}_{2-\mathrm{w}}$) is calculated by correcting for a 100 % water vapor pressure at 1 atm and by applying the virial equation of state (Weiss, 1974) as per the Guide to Best Practices for Ocean CO_2 Measurements (Dickson et al. 2007). The analyzer was calibrated daily by using pure N_2 as the zero concentration and a commercial gas mixture of 541 ppm CO_2 as span.

2.4 DOC, EDOC and GOC H'^{-1} measurements

Water samples for the analysis of EDOC and DOC were collected by using Niskin bottles attached to a rosette–CTD sampling system. For the surface microlayer, samples were collected from onboard a small boat drifting at a distance from the research vessel using a plate ocean microsurface sampler (Carlson, 1982). Briefly, two acid-washed perspex blades (50 cm long × 20 cm wide × 0.3 mm thick) were rinsed with surface seawater, gently inserted vertically into the water and then removed slowly; thereafter the microlayer water attached by surface tension was gently squeezed in between two Teflon blades. The water was collected in an acid-washed Teflon bottle and the maneuver repeated until 0.5 L of water was collected, typically after 30 min of two people working in parallel. When wind speed exceeded $20\,m\,s^{-1}$, this procedure could not be attempted for safety reasons. For the analysis of DOC, duplicate samples were collected in 10 mL pre-combusted (4.5 h, 500 °C) glass ampoules filled directly with water from the Niskin bottle, acidified to a pH < 2 by adding 15 µL of concentrated (85 %) H_3PO_4, sealed under flame, and stored until analysis in the laboratory with a Shimadzu total organic carbon (TOC)-Vcsh analyzer following standard non-purgeable organic carbon (NPOC) analysis (Spyres et al., 2000). Standards of $2\,\mu mol\,C\,L^{-1}$ and $44\,\mu mol\,C\,L^{-1}$ (provided by D. A. Hansell and W. Chen from the University of Miami) were used to assess the accuracy of our estimates. EDOC and GOC samples were collected following the procedure described by Dachs et al. (2005) and Ruiz-Halpern et al. (2010). For GOC samples, filtered air (collected upstream from the boat to avoid contamination from in situ emissions) was bubbled for approximately 30 min in 50 mL of high-purity Milli-Q water acidified to a pH < 2 with concentrated (85 %) H_3PO_4. Defining the dimensionless Henry's law constant (H') as the ratio of the concentrations in the gas phase and dissolved phase, this procedure allows for estimation of the concentrations of organic carbon equilibrated with the gas-phase organic carbon (GOC H'^{-1}). EDOC measurements were obtained by bubbling 1 L of sampled unfiltered seawater with high-grade (free of carbon) N_2 for 8 min, which we determined sufficient to reach equilibrium. The stream of gas with the evolved EDOC is redissolved in 50 mL of acidified, high-purity Milli-Q water, as with GOC H'^{-1}. The unfiltered seawater was gently siphoned from a Niskin bottle to a 1 L pre-combusted (4.5 h, 500 °C) glass bottle to avoid turbulence of the sample water and minimum contact with the atmosphere. Finally, EDOC and GOC H'^{-1} samples were stored in pre-combusted (4.5 h, 500 °C) glass ampoules, which were then sealed under flame, until analysis in the laboratory as for DOC, but with the sparge gas procedure turned off in the Shimadzu total organic carbon TOC-Vcsh instrument (Dachs et al., 2005; Ruiz-Halpern et al., 2010). EDOC and GOC H'^{-1} concentrations were corrected for contamination by subtraction following the analysis of blanks, obtained by directly bubbling the high-purity acidified Milli-Q water with high-grade N_2 without the sample water after collection of each set of EDOC and GOC at the stations. Blank levels reflect the concentration of CO_2 equilibrated with water at the low temperatures of the Southern Ocean waters. The recoveries of the EDOC analysis were evaluated for acetone, and were 31 % for the ICEPOS cruise. These values are lower than previously reported due to the low temperatures of seawater. However, since EDOC and GOC comprise an undetermined amount of compounds with different volatility, recoveries may be higher for compounds with higher values of the Henry's law constant.

2.5 Chlorophyll *a* (Chl *a*) and krill determination

Chl *a* concentration was determined spectrofluorimetrically (Parsons et al., 1984) for water samples collected from Niskin bottles at several depths. Chl *a* concentration was determined by filtering 50 mL samples onto 25 mm diameter Whatman GF/F filters at each station. After filtration, the filters were placed in tubes with a 90 % acetone solution for 24 h to extract the pigment. Chl *a* fluorescence was measured in a Shimadzu RF-5301 PC spectrofluorimeter, previously calibrated with a pure solution of Chl *a*.

Krill abundance was estimated by using a Simrad™ EK60 multifrequency echosounder. Working frequency was 38 kHz with a 256 µs sampling interval, 1024 µs pulse duration and a bandwidth of 2425 Hz. The SonarData Echoview 4 software was used to process the data obtained. A maximum depth of 100 m and 80 dB of minimum target strength (TS), applying a time-varied gain (TVG) function, was used to identify the krill targets. Finally, the data were subjected to a 100 m depth cell and a 1 min duration analysis. The number of targets detected down to 100 m cells was counted at 1 min intervals and the volume sampled by the beam calculated (Ruiz-Halpern et al., 2011).

2.6 Meteorological and seawater data

Pressure, wind speed (U_{10}), air temperature and solar radiation (from a Aanderaa meteorological station) fluorescence, sea-surface temperature (SST), and salinity (Sal) (from a Seabird SBE 21 thermosalinograph) were continuously measured and averaged at 1 min intervals. Fluorescence was positively correlated with Chl *a* ($r = 0.74$, $p < 0.05$), allowing for the use of fluorescence measurements as a proxy for phytoplankton abundance. Pitch, roll and heading of the research vessel were also recorded at 1 min intervals and used in a routine embedded in the software, integrating navigation and meteorological data to correct the wind speed data from the ship movement and flow distortion. The corrected wind velocities were then extrapolated to the wind velocity at 10 m (U_{10}) by using the following logarithmic expression: $U_{10} = U_z\,[0.097\ln(z/10)+1]^{-1}$, where z is the height of the wind sensor position (Hartman and Hammond, 1985).

2.7 Flux calculations

Diffusive air–seawater exchange of CO_2 was estimated by using the wind speed dependence of the mass transfer velocity (k_{600}) from instantaneous wind speeds (U_{10}, $m\,s^{-1}$) following the expression $k_{600} = 0.222\ \ U_{10}^2 + 0.333U_{10}$

(Nightingale et al., 2000). The calculation of air–seawater CO_2 flux (F_{CO_2}) used the expression (Eq. 1)

$$F_{CO_2} = k_w \times S \times \Delta f CO_2, \quad (1)$$

where $\Delta f CO_2$ is the difference between CO_2 fugacity in the surface of the ocean and that in the lower atmosphere ($\Delta f CO_2 = f CO_{2-w} - f CO_{2-a}$); k_w, the gas transfer coefficient, was normalized to a Schmidt number of 600 at in situ temperature and salinity ($k_w = k_{600} \times (600/Sc)^{0.5}$); and S is the CO_2 solubility coefficient, calculated from seawater temperature and salinity (Weiss, 1974). Likewise, OC net diffusive fluxes (F_{AW}) were estimated as the sum of gross volatilization ($F_{Vol} = k_{aw} \times$ EDOC) and absorption ($F_{Ab} = -k_{aw} \times$ GOC H'^{-1}), where k_{aw} is the gas transfer velocity for exchangeable OC estimated from k_{600} values and Schmidt numbers assuming an average molecular weight (MW) of GOC of 120 g mol^{-1} (Dachs et al. 2005). The fluxes are estimated by considering the air–water mass transfer coefficient (k_{AW}) as given by

$$\frac{1}{k_{AW}} = \frac{1}{k_w} + \frac{1}{k_A H'}, \quad (2)$$

where k$_W$ is the water-side mass transfer coefficient estimated from Nightingale et al. (2000) and scaled by the Schmidt number as previously described, and k_A is the air-side mass transfer coefficient that can be estimated from the k'_A value for water vapor in air (Schwarzenbach et al. 2003) by means of

$$k'_A = (0.2U_{10} + 0.3)\,864, \quad (3)$$

$$k_A = k'_A \left(\frac{D_A}{D_{A,H_2O}}\right)^{0.61}, \quad (4)$$

where 864 is the conversion factor from cm s^{-1} to m d^{-1}, D_A is the diffusivity of GOC or EDOC in air, and D_{A,H_2O} is the diffusivity of water vapor in air. This estimation methodology is widely used for the estimation of the air–water mass transfer coefficients of semivolatile compounds (Scwarzenbach et al., 2003; Dachs et al., 2002). Just for clarification, we define H' as the ratio of vapor pressure over solubility in water. The opposite criterion is used in part of the literature for volatile compounds, but this is how it is usually defined for semivolatile compounds (Schwarzenbach et al., 2003). For chemicals with $H' > 0.05$, k_{AW} is approximately equal to k_W. Because there is a wide range of H' in the mix of EDOC and GOC H'^{-1}, we have calculated volatilization and absorption fluxes with a range of H' spanning three orders of magnitude (0.0005, 0.005, 0.05). Details for the associated uncertainties derived from the use of an average MW are given in Ruiz-Halpern et al. (2010).

The ICEPOS cruise delivered 61 coupled measurements of exchangeable organic carbon in water and air, whereas only 20 and 25 were obtained during ESASSI and ATOS-Antarctica cruises, respectively (Fig. 1). To characterize the stations sampled and to compare CO_2 and exchangeable organic carbon fluxes, hourly averages of SST, Sal, (U_{10}), $f CO_{2-w}$, $f CO_{2-a}$ and $F CO_2$ were calculated centered around (±30 min) the time EDOC and GOC H'^{-1} estimates were collected.

3 Results

3.1 Meteorological conditions and seawater column properties

The spatial distribution of the three cruises in the three different years is shown in Fig. 2 and the mean values for every station by area and cruise (year) are shown in Table 1. The wind pattern was spatially variable, from lower velocities in sheltered areas to values higher than 20 m s^{-1} at some locations (Fig. 2a). Sea-surface temperature was close to 0 °C in the northeastern sector of the Antarctic Peninsula, close to the Antarctic Sound, and in the northern sector of the Weddell Sea, whereas higher values were observed in the western sector of the Antarctic Peninsula (Fig. 2b). The salinity pattern was less variable; the higher values were located to the north of the Antarctic Peninsula, between 60 and 50°W, whereas the lower values were found in the western sector of the Antarctic Peninsula and eastern limb of the domain (Fig. 2c).

In spite of the spatial variability, the mean wind speeds were quite constant among the areas and for the three different cruises (years), ranging between 7 m s^{-1} in the western sector of the Antarctic Peninsula and 8 m s^{-1} in Bransfield Strait and Weddell Sea sector. Mean sea-surface temperature was close to 0 °C in the Weddell Sea sector of the sampled domain but higher, around 1.5 °C, in Bransfield Strait and the western sector of the Antarctic Peninsula. However, the temperature range exceeded 4 °C, as a minimum of −1.1 °C and a maximum temperature of 3.2 °C were recorded in the Bellingshausen Sea during the ATOS-Antarctica cruise. On average, the most saline sea-surface water was found during the ESASSI cruise, in the Weddell–Scotia confluence (34.2), whereas the less saline was observed in the western sector of the Antarctic Peninsula (33.4). However, a maximum salinity of 34.43 was recorded in ICEPOS at Bransfield Strait and a minimum of 32.53 in the Bellingshausen Sea during ATOS-Antarctica. In general, the most saline waters were associated with higher temperatures, especially in the northern limb of the sampled domain, leading to a reduction in the solubility of CO_2.

Table 1. Mean ± standard error (SE), median and ranges for the physical and biological parameters measured at the stations where coupled EDOC–GOC measurements were taken. Data for all three cruises: ICEPOS in 2005, ESASSI in 2008 and ATOS-Antarctica in 2009. Data were grouped into cruises and areas. Note that means for the different areas were estimated from the three cruises. There were no acoustic data to estimate krill density for the ESASSI cruise.

Surface	SST °C	Sal	U $m\,s^{-1}$	Chl *a* $mg\,m^{-3}$	Krill density 10^{-6} ind m^{-3}
Cruise					
ICEPOS	1.40 ± 0.09	33.70 ± 0.05	8.2 ± 0.5	2.4 ± 0.3	85 ± 8
	1.70 [(−0.4)–(+2.1)]	33.80 [32.7–34.4]	8.6 [0.5–16.9]	2.2 [0.5–4.6]	72 [27–260]
ESASSI	0.32 ± 0.13	34.21 ± 0.04	7.4 ± 0.7	0.8 ± 0.1	no data
	0.25 [(−0.5)–(+1.5)]	34.28 [33.75–34.38]	7.4 [1.7–11.9]	0.85 [0.17–1.27]	
ATOS	1.30 ± 0.20	33.80 ± 0.09	6.6 ± 0.5	3.9 ± 1.4	66 ± 6
	1.62 [(−1.1)–(+3.18)]	33.80 [32.5–34.33]	6 [2.7–11.6]	1.68 [0.11–31.6]	62 [19–160]
Area					
Weddell Sea sector	0.09 ± 0.08	34.12 ± 0.05	8.1 ± 0.6	3.6 ± 1.6	59 ± 7
	0.02 [(−0.47)–(+0.96)]	33.81 [32.74–34.43]	7.8 [1.7–13.3]	2.2 [0.5–4.6]	72 [27–260]
Bransfield Strait	1.61 ± 0.09	33.98 ± 0.03	8.1 ± 0.6	2.6 ± 0.4	110 ± 11
	1.75 [(−0.17)–(+2.76)]	33.90 [33.70–34.40]]	8.2 [0.5–16.9]	2.41 [0.33–7.7]	81 [20–260]
Western sector of the Antarctic Peninsula	1.50 ± 0.80	33.40 ± 0.30	7.0 ± 3.0	1.7 ± 0.7	60 ± 50
	1.72 [(−1.1)–(+3.18)]	33.40 [32.50–33.80]	6.3 [2.4–12.7]	1.16 [0.12–4.55]	56 [19–160]

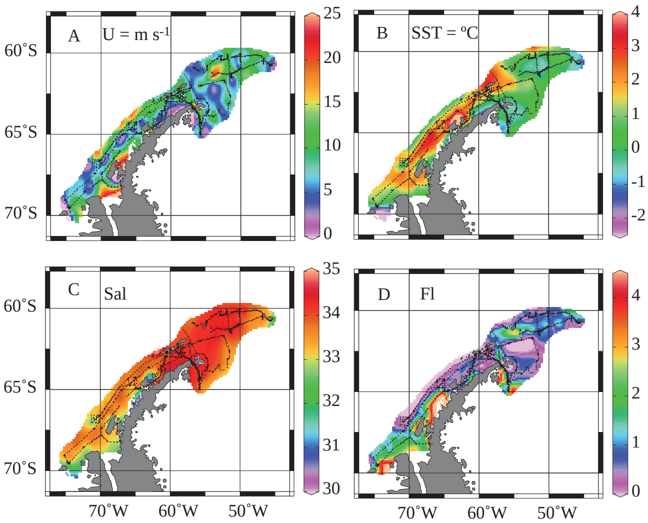

Figure 2. The distribution of shipboard continuous measurements (all three cruises combined) of wind speed (U, $m\,s^{-1}$, **A**), sea-surface temperature (SST, °C; **B**), salinity (Sal, **C**) and fluorescence (Fl, **D**).

3.2 Chlorophyll *a* and krill distribution

Table 1 also reports the mean values for biological parameters. Chl *a* concentrations ranged greatly (Fig. 2d), with differences of up to two orders of magnitude in Chl *a* concentration among stations (Table 1). The highest mean Chl *a* concentration (3.9 mg Chl *a* m^{-3}, Table 1) was found in the Weddell Sea during the ATOS-Antarctica cruise, while the lowest mean Chl *a* concentration was found in the Weddell–Scotia confluence region during the ESASSI cruise (0.8 mg Chl *a* m^{-3}, Table 1). The lowest Chl *a* record was 0.12 mg Chl *a* m^{-3} in the Bellingshausen Sea during ATOS-Antarctica and an exceptionally high value of 31.66 mg Chl *a* m^{-3}, almost 300 times the minimum value, was also measured during ATOS-Antarctica, but in the Weddell Sea (Table 1). Lower krill densities were observed in the western sector of the Antarctic Peninsula and on the Weddell Sea side. In Bransfield Strait the mean concentration was twice the mean value of the neighboring areas. A maximum of 2.6×10^{-4} individuals m^{-3} was found in Bransfield Strait during ICEPOS and a minimum of 1.9×10^{-5} individuals m^{-3} in the Bellingshausen Sea during ATOS-Antarctica.

3.3 CO_2 concentration and fluxes

The spatial distribution of the three cruises in the three different years is shown in Fig. 3 and the mean values for stations by area and cruise (year) are shown in Table 2. The fugacity of CO_2 in surface seawater (fCO_{2-w}) was also highly variable with minima near shore, at the western sector of the Antarctic Peninsula, to the east of the tip of the Antarctic Peninsula, and near the South Orkney Islands (Fig. 3a). Concurrently, fCO_{2-a} was less variable and displayed the opposite trend (Fig. 3b). The difference between both fugacities, ΔfCO_2, showed undersaturated areas along the coast of the Antarctic Peninsula, to the east of the peninsula, and next to the South Orkney Islands, the areas with the colder, less saline waters. However supersaturated areas were concentrated in the northern limb of the sampled domain and next to the South Shetland Islands, areas with warmer and

Table 2. Mean ± standard error (SE), median and ranges for CO_2 fugacity in water and air, EDOC, GOC H'^{-1} and DOC throughout the tracking of the three cruises ICEPOS in 2005, ESASSI in 2008 and ATOS-Antarctica in 2009. Data were grouped into cruises and basins. Note that means for the different areas come from all three cruises and that there are no DOC data for the ESASSI cruise.

Surface	$f\mathrm{CO}_{2-\mathrm{w}}$ µatm	$f\mathrm{CO}_{2-\mathrm{a}}$ µatm	EDOC µmol C L^{-1}	GOC H'^{-1} µmol C L^{-1}	DOC µmol C L^{-1}
Cruise					
ICEPOS	368 ± 10	356 ± 1	36 ± 4	35 ± 3	54 ± 1
	374 (183–475)	357 (345–374)	27 (0–147)	29 (11–134)	54 (45–63)
ESASSI	396 ± 8	357 ± 1.4	40 ± 8	43 ± 9	no data
	400 (271–440)	358 (345–366)	31 (0–125)	34 (9–136)	
ATOS	341 ± 13	367 ± 1.4	60 ± 5	73 ± 5	62 ± 7
	364 (148–416)	367 (350–379)	57 (1–102)	70 (16–104)	54 (45–181)
Area					
Weddell Sea sector	346 ± 16	360 ± 1.4	49 ± 7	40 ± 5	71 ± 16
	387 (148–440)	360 (345–376)	42 (0–147)	30 (9–137)	56 (48.15–118.37)
Bransfield Strait	401 ± 6	360 ± 1.0	39 ± 5	50 ± 4	54 ± 1
	389 (350–475)	359 (350–379)	34 (1–102)	44 (20–134)	53 (45–66)
Western sector of the	344 ± 7	356 ± 1.4	41 ± 6	47 ± 8	58 ± 5
Antarctic Peninsula	351 (282–419)	353 (346–372)	21 (0–98)	21 (11–100)	54 (45–107)
Total mean ± SE	367 ± 7	359 ± 0.8	43 ± 3	46 ± 3	59 ± 4

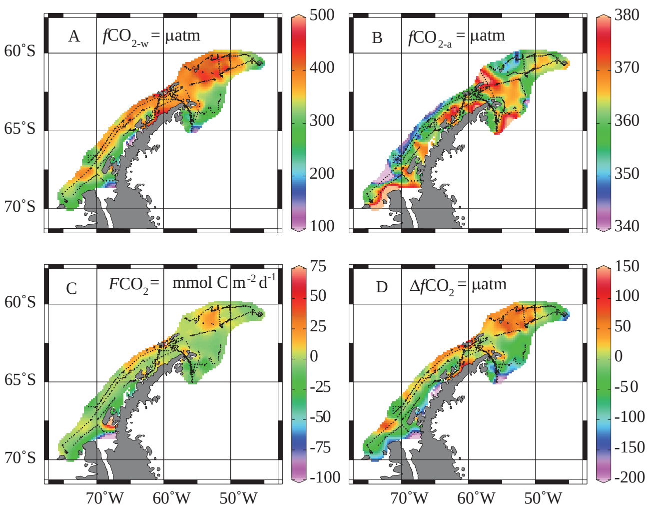

Figure 3. The distribution of shipboard continuous measurements (all three cruises combined) of $f\mathrm{CO}_{2-\mathrm{w}}$ (µatm, **A**), $f\mathrm{CO}_{2-\mathrm{a}}$ (µatm, **B**), F_{CO_2} (mmol C m^{-2} d^{-1}, **C**) and $\Delta f\mathrm{CO}_2$ (µatm, **D**).

more saline water (see Figs. 1 and 3d). $F\mathrm{CO}_2$ has a similar distribution to $\Delta f\mathrm{CO}_2$, except for a slight modulation due to the influence of wind speed in the flux calculations. This distribution supports oceanic CO_2 uptake along most of the sampled domain, except at the northern edge of the domain, the South Shetland Islands region, and several locations next to the Antarctic Peninsula that acted as a net source of CO_2 to the atmosphere (Fig. 3c).

Although the overall mean values of $f\mathrm{CO}_{2-\mathrm{w}}$ and $f\mathrm{CO}_{2-\mathrm{a}}$ were similar among cruises (years) and regions, the horizontal distribution showed high variability of $f\mathrm{CO}_{2-\mathrm{w}}$ (see Table 2). Sea-surface $f\mathrm{CO}_{2-\mathrm{w}}$ ranged from strong supersaturation in Bransfield Strait during ICEPOS to strong undersaturation in the Weddell Sea during the ATOS-Antarctica cruise (Table 2). Supersaturation values above 400 µatm were found in all cruises and areas, while the Weddell Sea sector of the domain presented the most undersaturated station by far (148 µatm), followed by a station located to the west of the Antarctic Peninsula (282 µatm). In Bransfield Strait, minima values were close to equilibrium (350 µatm for $f\mathrm{CO}_{2-\mathrm{w}}$ with the same value for $f\mathrm{CO}_{2-\mathrm{a}}$; see Table 2). $f\mathrm{CO}_{2-\mathrm{w}}$ in the temperature–salinity space showed, in general, higher values in the more saline, warmer waters (Fig. 4).

The net fluxes of CO_2 ($F\mathrm{CO}_2$; see Table 3) showed a distribution centered around equilibrium. A maximum of -39 mmol C m^{-2} d^{-1} of ocean carbon dioxide uptake was found in the Weddell Sea sector during the ICEPOS cruise, while the maximum emission of CO_2 to the atmosphere (27 mmol C m^{-2} d^{-1}) was calculated also during the ICEPOS cruise but in Bransfield Strait. Only in the western sector of the Antarctic Peninsula were there more stations showing a net CO_2 uptake, while CO_2 emissions were found in the Weddell Sea sector of the sampled domain and in Bransfield Strait for all the cruises.

Although there were no strong correlations, fugacity of CO_2 in the surface layer of the water column was strongly undersaturated in sites with high Chl *a* concentrations, and the sites more strongly supersaturated were those where the highest concentrations of krill were measured (Fig. 5). Two-thirds of the values represented net emission of CO_2 to the

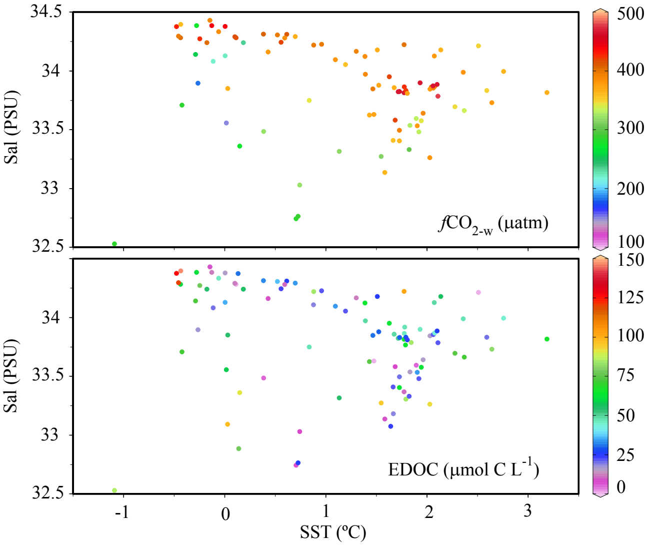

Figure 4. Temperature–salinity diagram color-coded for fCO_{2-w} and EDOC for all three cruises combined.

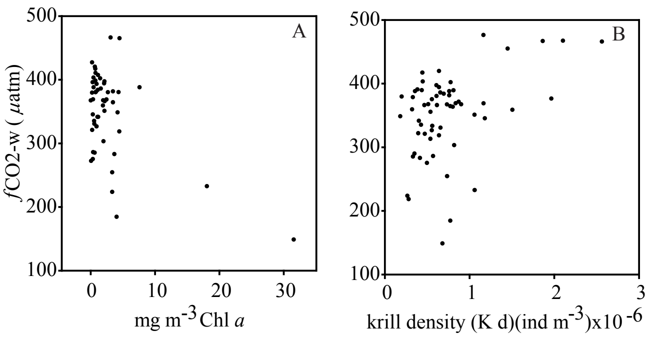

Figure 5. Scatterplots of surface (5 m) fCO_{2-w} vs. surface (5 m) Chl *a* **(A)** and krill density **(B)**. Data combined for all cruises and stations.

atmosphere (Fig. 6). Bransfield Strait presented 100 % supersaturated stations for CO_2, and only in the western sector of the Antarctic Peninsula were there more undersaturated stations than supersaturated ones (Table 3). Overall, FCO_2 distributions in the study area remained close to balance.

3.4 EDOC and GOC H'^{-1} distribution

Surface water EDOC, GOC H^{-1} and DOC were, on average, quite similar among cruises (years) and regions (Table 2). However, the spatial variability of EDOC and GOC H'^{-1} was high, with similar coefficients of variation (C.V.) for EDOC and GOC H'^{-1} (388 and 341 %, respectively), ranging from virtually no EDOC present in surface waters at some stations to a maximum of 147 µmol C L^{-1}; GOC H'^{-1} ranged between 9 and 137 µmol C L^{-1} among stations (Table 2). Despite this variability, around 60 % of both EDOC and GOC H'^{-1} concentrations comprised between 10 and 50 µmol C L^{-1} (see Fig. 7). In contrast, DOC values were less variable, with a DOC mean value of 59 ± 4 µmol C L^{-1} (Table 2) and a C.V. of 37 %, with only two stations with values above 100 µmol C L^{-1}. The distribution of EDOC in the temperature–salinity space did not follow the same pattern as for fCO_{2-w} (Fig. 4) and there was no apparent trend, since concentrations are reported in µmol C L^{-1}, which is independent of the effects of temperature and salinity. Table 3 presents the air–seawater exchange of OC (F_{AW}) at three different H' values spanning three orders of magnitude. For simplicity we discuss and compare the fluxes estimated at $H' = 0.0005$, since it is the most likely value in a cold water environment. F_{AW} were similar to those of CO_2, both in magnitude and direction. In general, the majority of stations showed oceanic uptake of exchangeable OC among cruises (years) and areas, except for the Weddell Sea sector (with 41 %) and ICEPOS, (with 18 %) having net fluxes towards the ocean. During the ESASSI cruise there was a balance between uptake and release of exchangeable OC. In fact, the strongest sink for OC was found during the ESASSI cruise and reached -58 mmol C m^{-2} d^{-1}, over the Weddell–Scotia confluence region. The strongest OC emission from the ocean (70 mmol C m^{-2} d^{-1}) was obtained on the Weddell Sea side during the ICEPOS cruise.

EDOC was independent ($p > 0.05$) of fCO_{2-w}, SST or Sal, and no significant relationship was found between EDOC or F_{AW} with Chl *a* or krill density ($p > 0.05$). There was no correspondence between EDOC and SML and a very weak relationship between GOC H'^{-1} and EDOC (Fig. 8), but during ICEPOS, EDOC values sampled in the surface microlayer (11 stations spanning along most of the cruise track) correlated linearly with EDOC concentrations – measured at 5 m depth ($R^2 = 0.55$, $p < 0.05$, Fig. 7).

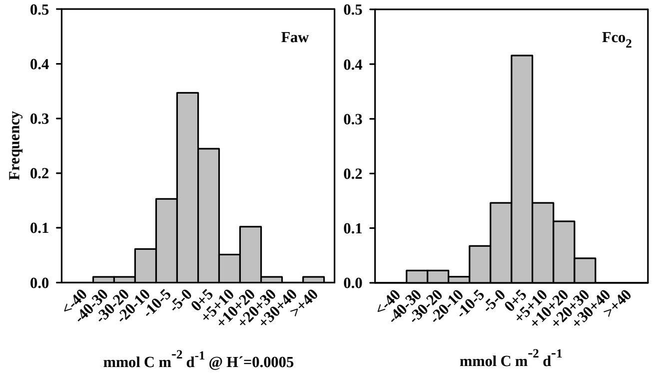

Figure 6. Frequency distribution of air–sea fluxes of exchangeable organic carbon (F_{aw}) and F_{CO_2} (mmol m^{-2} d^{-1}). Data binned in 10 mmol C m^{-2} d^{-1} intervals except close to 0, where it was binned in 5 mmol C m^{-2} d^{-1}.

Table 3. Mean ± standard error (SE), median and ranges for fluxes of organic carbon (F_{vol}, gross volatilization; F_{ab}, gross absorption; F_{aw}, net OC air–seawater exchange) for three different H' values (0.0005, 0.005, 0.05), and CO_2 (F_{CO_2}) throughout the track of the three cruises, ICEPOS in 2005, ESASSI in 2008 and ATOS-Antarctica in 2009. Data were grouped into cruises and areas. The percentage of stations with undersaturated CO_2 and OC uptake by the ocean are also shown.

Surface	H'	F_{vol} mmol C m^{-2} d^{-1}	F_{ab} mmol C m^{-2} d^{-1}	F_{aw} mmol C m^{-2} d^{-1}	F_{CO_2} mmol C m^{-2} d^{-1}	CO_2 uptake % stations	OC uptake % stations
Cruise							
ICEPOS	0.0005	11 ± 2 8[0.3–70]	−10 ± 1 −8[−28–(−0.6)]	1.4 ± 2 −1.1[−18–(+60)]	1.4 ± 2 2.3[−39–(+27)]	27	18
	0.005	55 ± 9 37[0.5–395]	−50 ± 5 −39[−166–(−0.8)]	14 ± 15 −6[−207–(+640)]			
	0.05	95 ± 16 61[0.5–741]	−86 ± 10 −66[−322–(−0.84)]	77 ± 8 −4.8[−106–(+342)]			
ESASSI	0.0005	11 ± 3 5[0.1–53]	−14 ± 4 −6[−58–(−2.3)]	−2.5 ± 2 −0.03[−33–(+12)]	6.4 ± 1.7 4.1[−5–(+21)]	10	50
	0.005	53 ± 17 25[0.3–285]	−70 ± 21 −24[−311–(−5)]	−13 ± 12 −0.07[−170–(+56)]			
	0.05	87 ± 31 34[0.5–508]	−118 ± 37 −33[−553–(−5.5)]	−23 ± 21 −0.05[−286–(+93)]			
ATOS	0.0005	15 ± 2 14[0.9–34]	−18 ± 10 −14[−40–(−3.8)]	−2.6 ± 1 −2[−21–(+11)]	−2 ± 1.4 0.05[−20–(+13)]	46	88
	0.005	68 ± 10 58[3.5–189]	−80 ± 2 −57[−225–(−16)]	−12 ± 6 −8[-92–(+43)]			
	0.05	107 ± 18 84[5–350]	−126 ± 21 −83[−414–(−23)]	−19 ± 10 −14[−150–(+60)]			
Basin							
Weddell Sea	0.0005	15 ± 3 9[0.1–70]	−14 ± 3 −8[−58–(−2.3)]	1.5 ± 3 0.5[−34–(+60)]	−2.1 ± 3 [−39–(+21)]	38	41
	0.005	73 ± 17 44[0.4–396]	−68 ± 15 −39[−311–(−5)]	9 ± 17 2.2[−170–(+343)]			
	0.05	1234 ± 32 68[0.5–740]	−114 ± 26 −68[−553–(−6)]	17 ± 30 3.3[−286–(+640)]			
Bransfield Strait	0.0005	12 ± 1.2 10[0.4–34]	−14 ± 1.3 −13[−40–(−0.6)]	−2.3 ± 1 −1.8[−18–(+14)]	6.9 ± 1.22 4.2.3(0–23)	0	71
	0.005	58 ± 7.4 52[0.5–190]	−71 ± 7.4 −57[−224–(−0.8)]	−11 ± 5.2 −7[−106–(+91)]			
	0.05	100 ± 14 79[0.5–399]	−121 ± 14 −102[−414–(−0.84)]	−17 ± 9.7 −11[−207–(+196)]			
Bellingshausen Sea	0.0005	10 ± 2 6.5[1.1–28]	−9 ± 1 −7[-37–(−1.3)]	0.9 ± 2 −1[−19–(+18)]	−1.5 ± 0.78 −1.7[−9–(+6)]	56	55
	0.005	42 ± 7 26[3.6–150]	−39 ± 7 −31[−197–(−3.4)]	3.4 ± 7 −3.3[−92–(+86)]			
	0.05	64 ± 12 40[4.6–268]	+62 ± 12 −45[−352–(−4)]	4.2 ± 11 −4[−150–(+140)]			
Total mean ± SE	0.0005 0.005 0.05	12 ± 1 58 ± 6 96 ± 12	−13 ± 1 −61 ± 6 −102 ± 10	−0.3 ± 1 −1.1 ± 6 −1.5 ± 10	1.6 ± 1.2	27	58

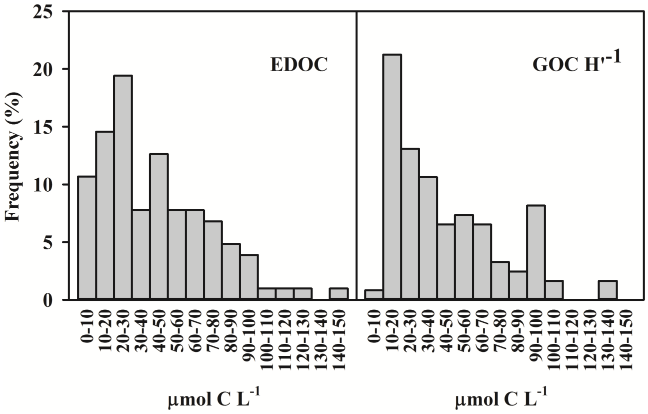

Figure 7. Frequency distribution of surface EDOC (median 34 µmol C L^{-1}) and GOC H'^{-1} (median 36 µmol C L^{-1}) for all three cruises.

3.5 Depth profiles and diel cycles

A total of 27 vertical profiles were performed (see table in the Supplement for details on depths and concentrations of each profile), 5 during ICEPOS and 22 during ATOS-Antarctica. Figure 9 contains representative examples of depth profiles of EDOC and Chl *a* from two cruises, with 10 of these profiles showing an agreement between OC and Chl *a* (Fig. 9a and b); 4 profiles of OC showed an opposite pattern to that of Chl *a* (Fig. 9c) and 13 showed no clear pattern (Fig. 9d). A Pearson chi-squared (X^2) analysis showed these profile relationships to be different than expected by chance ($X^2 = 15.5$, $p < 0.001$).

The diel cycles performed during ICEPOS – from 3–5 February, 13–14 February and 16–18 February 2005 – showed, in general, two distinct peaks around midday and midnight for EDOC, while GOC H'^{-1} showed no diel variability (Fig. 10). Sea-surface temperature and salinity were overplotted with CO_2 fugacities to analyze whether their changes are correlated during the ICEPOS cruise. Note that the overall sampling, including also ATOS and ESASSI cruises, accounts for the northeastern sector of the Antarctic Peninsula, the South Scotia Ridge, Bransfield Strait and the western sector of the Antarctic Peninsula, as well as coastal areas where ice-formation–melting processes take place. All these areas show different, local variations of Antarctic Surface Water and/or Shelf Water. In particular, ICEPOS crossed several of these areas along their tracking. fCO_{2-a} values remained almost constant ($\sim$ 360 µatm) during the ICEPOS cruise, while fCO_{2-w} showed a higher degree of variability. In general, when fCO_{2-w} values were higher ($>$ 400 µatm), sea-surface temperature was relatively warm (around 2 °C) and salinity was around 33.8 (Fig. 11). One peak was observed at sunset during the 3–5 February period, one at nighttime and another at midday during the 13–15 February period, and a continuous one during night and day during the first part of the 16–18 February period (Fig. 11).

4 Discussion

4.1 Water column biological properties

The oceanographic properties of the Antarctic Peninsula depict this region as a highly dynamic and complex area, where several water masses with distinct characteristics are encountered (Mura et al., 1995). The cruises took place in the same season, albeit in different years. The ICEPOS and ATOS cruises overlapped in parts of their cruise tracks, whereas ESASSI took place a month earlier in austral summer of 2008 and was restricted to the Weddell–Scotia confluence region (Fig. 1). The mean and median values for the cruise data sets are remarkably similar, with small interannual variability, for most of the properties shown in this study, particularly the physical characteristics at the air–sea-surface interface. The western sector of the area sampled was, in general, warmer and less saline (Fig. 2), which held high values of fCO_{2-w} ($fCO_{2-w} > 400$ µatm around a temperature value of 2 °C and a salinity value of 33.8, and EDOC values were small; Fig. 4), favoring the flux of CO_2 towards the atmosphere, compared to colder, less saline areas. Moreover, high values of fCO_{2-w} were also observed when surface water is colder but saltier; this tendency can be seen in the SST vs. salinity diagram (Fig. 4; see Bransfield Strait and South Scotia Ridge regions in Figs. 2 and 3). At the time of sampling, some of the stations had an elevated content of Chl *a* and showed bloom conditions. This feature was also present close to the Antarctic Sound and close to the South Orkney Islands. These less saline waters are derived from the melting of the ice sheet during austral summer, as well as fresh water delivery from meltwater close to shore, and the accumulation of icebergs from the Weddell Sea in the South Orkney Islands, which has been shown to stimulate phytoplankton growth (Smith Jr. et al., 2007). Late spring and summer blooms are indeed controlled by abiotic factors as well as grazing pressure, and are generally found in the marginal ice zone (Lancelot et al., 1993; Arrigo et al., 1998).

The large variability in Chl *a* concentrations, spanning two orders of magnitude, corroborates the patchy nature in the distribution of phytoplankton characteristic of Antarctic waters (Priddle et al., 1994). Krill density also displayed a patchy distribution, in agreement with previous observations (Murray, 1996). The sparse data set presented here, and the active swimming behavior of krill swarms compared to free-floating phytoplankton, did not allow us to find any relationship between krill abundance and Chl *a* concentration, contrary to previous studies of long-term, high-spatial-resolution data sets analyzed by Atkinson et al. (2004).

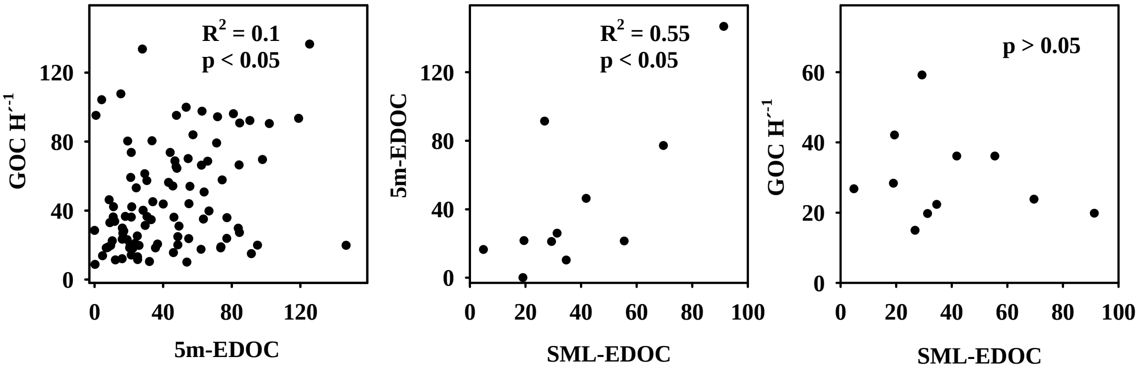

Figure 8. Relationship between GOC H'^{-1} and EDOC at 5 m depth (left panel), relationship between EDOC at 5 m depth and EDOC in the surface microlayer (SML-EDOC) (middle panel) and the relationship between GOC H'^{-1} and SML-EDOC (right panel).

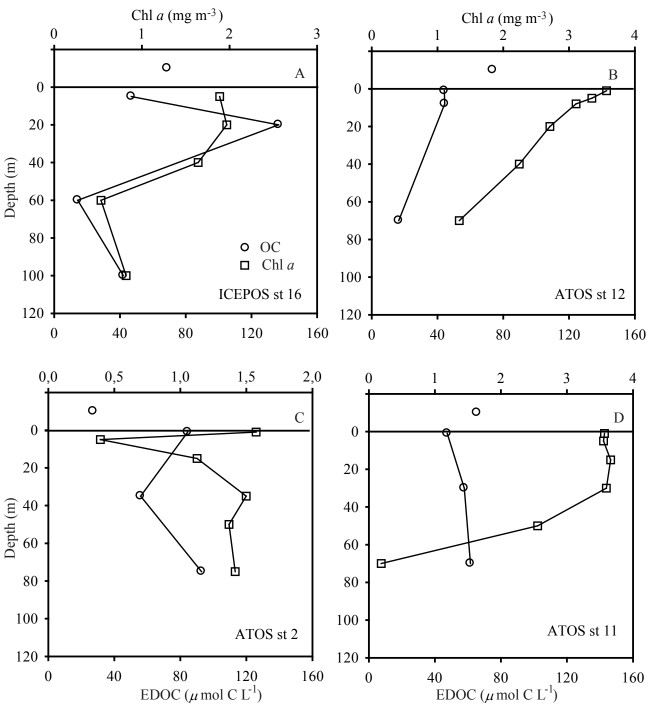

Figure 9. Representative depth profiles of EDOC and Chl a. Example profile performed during ICEPOS **(A)**. During ATOS-Antarctica, 9 followed Chl a **(B)**, 10 showed no clear pattern **(C)** and 3 were opposite to Chl a **(D)**. Open circles refer to organic carbon (OC) measured as EDOC in the water and as GOC H'^{-1} (single open circle) in the atmosphere. Open squares refer to Chl a.

4.2 CO_2 fluxes

The spatial variability of CO_2 concentration in the sea-surface layer was affected both by physical as well as biological factors. The colder, less saline waters from melting had, in general, lower fCO_{2-w} (Fig. 4) as a result of increased solubility of CO_2. Furthermore, meltwater may deliver nutrients and enhance phytoplankton growth, which would further draw down the amount of CO_2 available for exchange. The phytoplankton and krill abundance relationships were as expected: stations with the highest concentrations of Chl a supported the strongest undersaturation of CO_2, whereas stations were strongly supersaturated in CO_2 where krill abundance was highest (Fig. 5). Indeed, krill not only consumes phytoplankton, hence decreasing carbon fixation rates by algae, but also remineralizes organic matter back to CO_2 through respiration (Mayzaud et al., 2005). However, the relationships between CO_2 and the spatial heterogeneity in Chl a and krill were weak and driven by extremes. As CO_2 is a slow-diffusing gas, these relationships are expected to be weak, since krill is highly mobile and the partial pressure of CO_2 would average out physical and biological processes over longer timescales not captured by the survey conducted here.

The fugacity of CO_2 in air, fCO_{2-a}, although less variable (approximately between 350 and 380 µatm, a range of less than 30 µatm; see Table 2), showed a distribution opposite to that of fCO_{2-w} (Fig. 3a and b). The direction and potential intensity of carbon dioxide flux is determined by the gradient between air and seawater fugacities, ΔfCO_2. Therefore, on a small scale, regional variability in atmospheric CO_2 can lead to variability in air–seawater fluxes. This possibility, however, requires additional research, since most global estimates of air–sea CO_2 fluxes are based on regional mean atmospheric CO_2 values (Takahashi et al., 1997; Takahashi et al., 2009). Wind speed, which has been postulated to have a larger effect on CO_2 fluxes in the coastal ocean (Nightingale et al., 2000) and is forecast to increase in the future (Young et al., 2011), exerted a strong modulation in the intensity of observed air–sea CO_2 fluxes.

Hourly averaged FCO_2 data point to a prevalence of net efflux of CO_2 to the atmosphere (1.6 ± 1.2 mmol C m^{-2} d^{-1}), observed in 72 % of stations (Table 3, Fig. 5). However, the cruise track was not a random transit through the region, and therefore the statistics of hourly averaged do not necessarily represent the regional patterns. The range in fluxes is widened when no hourly

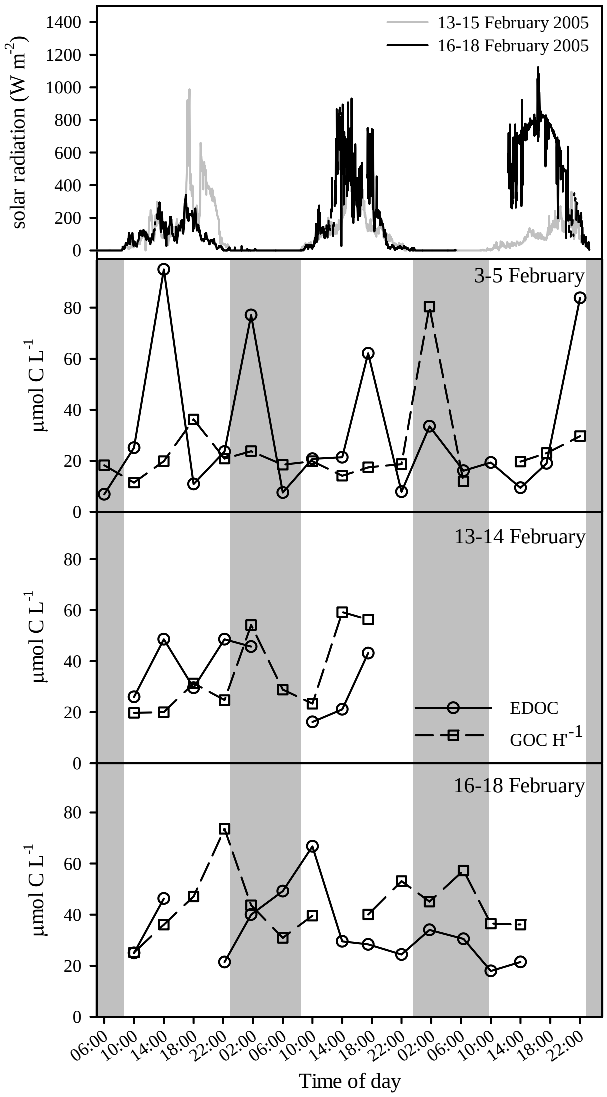

Figure 10. Diel variability of EDOC (solid line, open circles) and GOC H'^{-1} (dashed line, open squares). The top panel shows solar radiation for the different days sampled; data for the 3–5 February cycle are missing due to equipment failure.

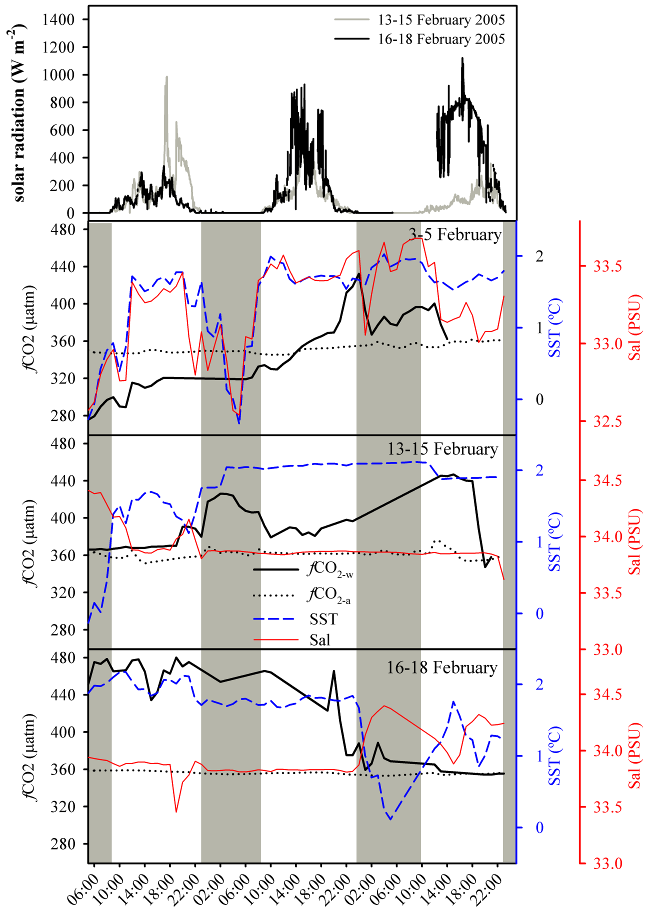

Figure 11. Diel variability of fCO_{2-a}, fCO_{2-w}, SST and salinity. The top panel shows solar radiation for the different days sampled; data for the 3–5 February cycle are missing due to equipment failure.

averaging was performed (Fig. 3c). There was a maximum emission to the atmosphere of $63.5\,mmol\,m^{-2}\,d^{-1}$, a maximum uptake of $-151.6\,mmol\,m^{-2}\,d^{-1}$ and a mean of $-0.3\,mmol\,m^{-2}\,d^{-1}$. Mapping of FCO_2 data suggests marine waters around the Antarctic Peninsula to be highly variable, and high-resolution measurements are necessary to appropriately estimate regional fluxes (Fig. 3c, Table 3). The emission to the atmosphere in this region thus comes from several hotspots at specific locations of strong emissions of CO_2 to the atmosphere. These emissions may come from areas with low productivity where high heterotrophic metabolism could support these fluxes. Overall, the region was found to be in near balance (i.e., neutral) with a net flux near 0.

4.3 Organic carbon fluxes

Mean EDOC and GOC H'^{-1} in this region (see Table 2, Fig. 7) had similar values between cruises, with the interannual variability less important than the overall variability, and were remarkably consistent with the values observed in the mid-Atlantic (mean $40\,\mu mol\,C\,L^{-1}$, range 10 to $115\,\mu mol\,C\,L^{-1}$; see Dachs et al., 2005). This highlights the ubiquitous nature of this pool of carbon. The DOC values found in our study, with an overall mean surface DOC of $59 \pm 4\,\mu mol\,C\,L^{-1}$ (Table 2) consistent with previous reports (e.g., Kähler et al., 1997), points to Antarctic surface waters as those supporting the lowest DOC pool in the ocean. Furthermore, in some cases DOC concentrations were lower than actual EDOC values. The low values of DOC render EDOC concentrations, comparable to those found in other areas (Dachs et al., 2005; Ruiz Halpern et al., 2010), proportionately more important in Antarctic waters. EDOC amounts, on average, to 67 % of the DOC present (Table 2), whereas in the mid-Atlantic and subarctic regions EDOC amounts only to 30–40 % of DOC (Dachs et al., 2005; Ruiz-Halpern et al., 2010). Because the EDOC pool is not included in the conventional measurements of DOC, which represents the non-purgeable fraction of dissolved organic matter (Spyres et al., 2000), these results indicate that neglecting the EDOC pool may be a particularly important gap in understanding the carbon cycle in Antarctic waters. Indeed, EDOC could represent a potentially important source of carbon to fuel microbial processes, since microbial communities are often limited by carbon concentrations in these environments (e.g., Bird and Karl, 1999), and several studies have demonstrated the use of VOCs and SOCs as a source of carbon for bacteria (Cleveland and Yavitt, 1998). However, experiments on the importance of the remineralization of EDOC for oceanic metabolism are still lacking.

There was no relationship between GOC H'^{-1} and SML-EDOC, and the relationship reported for the subtropical Atlantic and subarctic regions (Dachs et al., 2005; Ruiz-Halpern et al., 2010) between atmospheric (GOC H'^{-1}) and dissolved exchangeable organic carbon (EDOC) was weak in Antarctic waters (Fig. 7). This indicates that processes other than simple equilibrium mixing between these two pools control the relative partitioning of EDOC and GOC H'^{-1} in the water column and the atmosphere. Possible reasons to explain this weak relationship may come from more intense UV radiation in the Antarctic Peninsula (Madronich et al., 1998), affecting some of the volatile species present in the atmosphere and the SML by photochemical degradation (Zepp et al., 1998; Lechtenfeld et al., 2013) and chemical reactions with OH radicals (Bunce et al., 1991), the degree of EDOC released by phytoplankton through UV-induced cell lysis (Llabrés and Agustí, 2010) and subsequent photochemical degradation in the water column, or rapid bacterial usage of EDOC (Villaverde and Fernandez-Polanco, 1999). However, the positive relationship between 5 m depth EDOC and SML-EDOC (Fig. 8) provides support for a tight coupling between the processes occurring at 5m depth and those occurring at the ocean surface microlayer, which is not always the case (Calleja et al., 2005), implying rapid diffusion of organic carbon gases at small spatial scales. Unfortunately, this relationship does not currently allow us to assess the magnitude and direction of the flux of EDOC throughout the water column.

4.4 Depth profiles and diel cycles

The depth profiles of EDOC revealed the dynamic nature of this carbon pool (Fig. 9) and the participation of phytoplankton in the production of exchangeable organic carbon, consistent with its role as a source of DOC to the Antarctic marine environment (Ruiz-Halpern et al., 2011). Profiles also suggest active remineralization in the water column where other components, such as bacteria, may consume EDOC, since bacteria are often limited by carbon supply in Antarctica, where the DOC pool is particularly small (Kähler et al., 1997). Moreover, Antarctic krill has been recently demonstrated to release large amounts of DOC available to the microbial community (Ruiz-Halpern et al., 2011), and is likely to contribute to the EDOC pool as well, either mechanically, through sloppy feeding (Møller, 2007), or via direct excretion (Ruiz-Halpern et al., 2011).

The diel cycles performed provide further evidence of the dynamic nature of EDOC in the water column (Fig. 10). The relative invariance in the atmosphere of $f\mathrm{CO_{2-a}}$ and GOC H'^{-1} across the diel cycle suggests that it is EDOC and $f\mathrm{CO_{2-w}}$, as well as its horizontal inhomogeneity, the dominant factors controling the direction of the net carbon exchange and, under uniform wind speeds, for the variations in the magnitude of these fluxes. Peak EDOC concentrations were detected both at midday and in the middle of the dark period. These cycles point to a progressive buildup of EDOC in the water column as the day progresses: at midday, phytoplankton receives more light (both PAR and UV) and photosynthetic organic carbon production, and UV-induced damage accumulates; at midnight, the peak could possibly be related to krill's vertical migration patterns, initialized by an upward motion at dusk (Zhou and Dorland, 2004) and subsequent release of EDOC by sloppy feeding and excretion (Møller, 2005). However, as the cruise track traversed several water masses, these hypothesis remain speculative, and await further experimental tests. For $f\mathrm{CO_{2-w}}$, however, this pattern was less marked, with increased concentrations at night only on one occasion (13 February), and the changes observed can be attributed to the different physical properties of the local surface waters crossed along the ship tracking (Fig. 11).

5 Conclusions

The flux of volatile OC was predominantly towards the ocean (Table 3, Fig. 5), which corroborates previous reports of the ocean as a global sink for VOC and SOC (Dachs et al., 2005; Jurado et al., 2008; Ruiz-Halpern et al., 2010). However, a large portion (43 %) of the stations supported a net export of OC to the atmosphere, which has not been observed in the NE subtropical Atlantic or Greenland fjords, the other two areas where total VOC and SOC fluxes have been assessed (Dachs et al., 2005; Ruiz-Halpern et al., 2010). This dual source–sink nature for VOC and SOC suggests that VOC and SOC are emitted in some parcels of water and absorbed in others, providing a pathway for the rapid redistribution and transport of organic carbon within the ocean supplementing that mediated by water mass transport (Dachs et al., 2005). Provided the lack of terrestrial sources of organic matter in the Southern Ocean, it is likely that organic matter is redistributed across the ocean through atmospheric transport from source areas to sink areas. Moreover, the role of the atmosphere in the transport of marine organic carbon has not yet been addressed, but deserves further attention.

The data gathered during the three cruises in the Antarctic region provide compelling evidence for an important and dynamic role of volatile and semivolatile organic carbon in carbon cycling in the Southern Ocean, consistent with previous reports in the subtropical Atlantic (Dachs et al., 2005) and subarctic fjords (Ruiz-Halpern et al., 2010), as well as model calculations (Jurado et al., 2008).

EDOC pools in Antarctic marine waters may be comparatively more important than in other regions since they account for a larger proportion of total dissolved OC, with concentrations closely approaching those of (non-purgeable) DOC. Air–seawater EDOC fluxes are also important; however, variability in these fluxes resulted in air–seawater exchanges of organic carbon not too different from 0 when averaged across stations and cruises (Table 3), suggesting that emission and absorption of VOC and SOC represent pathways for transport and redistribution that are balanced across the region. While emission and uptake of VOC and SOC compounds may be in approximate balance in this region, the individual compounds are probably not, as some components of this flux, such as persistent organic pollutants or methanol (Yang et al., 2013), are likely to move predominantly from the atmosphere to the ocean, whereas some others, such as DMS, have oceanic sources and are expected to flow from the ocean to the atmosphere. Because the components of the flux originated in the ocean or the atmosphere are likely to have different properties, the flux remains significant even if, on a carbon basis, they are approximately in balance at the regional scale.

The net flux of organic carbon, comparable in magnitude to the flux of CO_2, is the result of a complex mixture of fluxes of different compounds. These compounds are also active in the atmosphere: they affect the radiative balance through greenhouse effects, the oxidative properties of the atmosphere, hydroxyl radical formation, ozone cycling and cloud and secondary aerosol formation. Likewise, little is known about the properties and possible effects of EDOC in the water column, as well as other possible producers other than micro- and macroalgae. EDOC in the water column is affected by several forcing factors, including temperature and salinity, that will affect their solubility. Biological processes in the water column, also affect EDOC concentrations. Phytoplankton would be involved in the production of EDOC together with bacteria (Kuzma et al., 1995), which can also act as a sink of VOC (Cleveland and Yavitt, 1998), as it has been demonstrated for the production and consumption of isoprene. Thus, by its remineralization, bacteria could contribute not only to the EDOC pool in the water column but also to CO_2 production. Moreover, the current ocean acidification scenario may influence EDOC concentrations by changing the volatility of some compounds (i.e., protonation), removing them from the EDOC pool and transferring them to the DOC pool.

In summary, the data presented here provide evidence of important air–sea fluxes of volatile and semivolatile species of organic carbon in the waters surrounding the Antarctic Peninsula, comparable in magnitude to air–sea CO_2 fluxes. Understanding the sources, sinks and cycling of volatile and semivolatile organic carbon is an imperative to understand the carbon budget of the ocean.

The Supplement related to this article is available online at doi:10.5194/bg-11-2755-2014-supplement.

Acknowledgements. We thank the commander and crew of the R/V *Hespérides* for dedicated and professional assistance, the personnel of the Unidad de Tecnología Marina (UTM) for highly professional technical support, Miquel Alcaráz for help with krill collections, Pedro Echeveste for Chl *a* analysis, and Amaya Álvarez-Ellacuría for her insight on MATLAB. This is a contribution of both Aportes Atmosféricos de Carbono Orgánico y Contaminanates al óceano Polar (ATOS) and the Spanish component of the Synoptic Antarctic Shelf-Slope Interactions study (ESASSI), funded by the Spanish Ministry of Science under the scope of the International Polar Year (IPY). Maria Ll. Calleja was funded by the Spanish Research Council (CSIC, grant JAEDOC030) and cofounded by the Fondo Social Europeo (FSO). We would also like to thank Mingxi Yang and Wiley Evans for their thorough and insightful comments during the review process of the manuscript, as it has now greatly improved from the initial version.

Edited by: K. Suzuki

References

Arrigo, K. R., Worthen, D., Schnell, A., and Lizotte, M. P.: Primary production in Southern Ocean waters, J. Geophys. Res., 103, 15587–15600, doi:10.1029/98JC00930, 1998.

Atkinson, A., Siegel, V., Pakhomov, E., and Rothery, P.: Long-term decline in krill stock and increase in salps within the Southern Ocean, Nature, 432, 100–103, doi:10.1038/nature02996, 2004.

Ayers, G. P. and Gillett, R. W.: DMS and its oxidation products in the remote marine atmosphere: implications for climate and atmospheric chemistry, J. Sea Res., 43, 275–286, 2000.

Bird, D. F. and Karl, D. M.: Uncoupling of bacteria and phytoplankton during the austral spring bloom in Gerlache Strait, Antarctic Peninsula, Aquat. Microb. Ecol., 19, 13–27, doi:10.3354/ame019013, 1999.

Bunce, N. J., Nakai, J. S., and Yawching, M.: A model for estimating the rate of chemical transformation of a VOC in the troposphere by two pathways: photolysis by sunlight and hydroxyl radical attack, Chemosphere, 22, 305–315, 1991.

Bravo-Linares, C. M., Mudge, S. M., and Loyola-Sepulveda, R. H.: Occurrence of volatile organic compounds (VOCs) in Liverpool Bay, Irish Sea, Mar. Pollut. Bull., 54, 1742–1753, doi:10.1016/j.marpolbul.2007.07.013, 2007.

Calleja, M. Ll., Duarte, C. M., Navarro, N., and Agustí, S.: Control of air-sea CO_2 disequilibria in the subtropical NE Atlantic by planktonic metabolism under the ocean skin, Geophys. Res. Lett., 32, L08606, doi:10.1029/2004GL022120, 2005.

Carlson, D. J.: A field evaluation of plate and screen microlayer sampling techniques, Mar. Chem., 11, 189–208, 1982.

Charlson, R. J., Lovelock, J. E., Andreae, M. O., and Warren, S. G.: Oceanic phytoplankton, atmospheric sulphur, cloud albedo and climate, Nature, 326, 655–661, 1987.

Clarke, A. and Leakey, R. J.: The seasonal cycle of phytoplankton, macronutrients, and the microbial community in a nearshore Antarctic marine ecosystem, Limnol. Oceanogr., 41, 1281–1294, 1996.

Cleveland, C. C. and Yavitt, J. B.: Microbial consumption of atmospheric isoprene in a temperate forest soil, Appl. Environ. Microbiol., 64, 172–177, 1998.

Cunliffe, M., Engel, A., Frka, S., Gašparović, B., Guitart, C., Murrell, J. C., Salter, M., Stolle, C., Upstill-Goddard, R., and Wurl, O.: Sea surface microlayers: A unified physicochemical and biological perspective of the air–ocean interface, Progr. Oceanogr., 109, 104–116, doi:10.1016/j.pocean.2012.08.004, 2013.

Dachs, J., Lohmann, R., Ockenden, W. A., Mejanelle, L., Eisenreich, S. J., and Jones, K. C.: Oceanic biogeochemical controls on global dynamics of persistent organic pollutants, Environ. Sci. Technol., 36, 4229–4237, 2002.

Dachs, J., Calleja, M. Ll., Duarte, C. M., Del Vento, S., Turpin, B., Polidori, A., Herndl, G. J., and Agustí, S.: High atmosphere-ocean exchange of organic carbon in the NE subtropical Atlantic, Geophys. Res. Lett., 32, L21807, doi:10.1029/2005GL023799, 2005.

del Giorgio, P. A. and Duarte, C. M.: Respiration in the open ocean, Nature, 420, 379–384, 2002.

Dickson, A. G., Sabine, C. L., and Christian, J. R. (Eds.): Guide to best practices for ocean CO_2 meausurements, PICES Special Publication, 3, 191 pp., 2007.

Doney, S. C., Fabry, V. J., Feely, R. A., and Kleypas, J. A.: Ocean acidification: the other CO_2 problem, Annu. Rev. Mar. Sci., 1, 169–192, doi:10.1146/annurev.marine.010908.163834, 2009.

Ducklow, H. W. and Doney, S. C.: What is the metabolic state of the oligotrophic ocean? A debate, Annu. Rev. Mar. Sci., 5, 525–533, doi:10.1146/annurev-marine-121211-172331, 2013.

Giese, B., Laturnus, F., Adams, F. C., and Wiencke, C.: Release of Volatile Iodinated C1–C4 Hydrocarbons by Marine Macroalgae from Various Climate Zones, Environ. Sci. Technol., 33, 2432–2439, doi:10.1021/es980731n, 1999.

Goldstein, A. H. and Galbally, I. E.: Known and Unexplored Organic Constituents in the Earth's Atmosphere, Environ. Sci. Technol., 41, 1514-1521, doi:10.1021/es072476p, 2007.

Gruber, N., Gloor, M., Fletcher, S. E. M., Doney, S. C., Dutkiewicz, S., Follows, M. J., Gerber, M., Jacobson, A. R., Joos, F., Lindsay, K., Menemenlis, D., Mouchet, A., Müller, S. A., Sarmiento, J. L., and Takahashi, T.: Oceanic sources, sinks, and transport of atmospheric CO_2, Global Biogeochem. Cy., 23, GB1005, doi:10.1029/2008GB003349, 2009.

Hansell, D. A. and Carlson, C. A. (Eds.).: Biogeochemistry of marine dissolved organic matter, Academic Press, 2002

Hardy, J. T.: The sea surface microlayer: biology, chemistry and anthropogenic enrichment, Progr. Oceanogr., 11, 307–328, 1982.

Hartman, B. and Hammond, D. E.: Gas exchange in San Francisco Bay, Hydrobiologia, 129, 59–68, 1985.

Hauser, E. J., Dickhut, R. M., Falconer, R., and Wosniak, A. S.: Improved method for quantifying the air-sea flux of volatile and semi-volatile organic carbon, Limnol. Oceanogr.-Methods, 11, 287–297, doi:10.4319/lom.2013.11.287, 2013.

Heald, C. L., Goldstein, A. H., Allan, J. D., Aiken, A. C., Apel, E., Atlas, E. L., Baker, A. K., Bates, T. S., Beyersdorf, A. J., Blake, D. R., Campos, T., Coe, H., Crounse, J. D., DeCarlo, P. F., de Gouw, J. A., Dunlea, E. J., Flocke, F. M., Fried, A., Goldan, P., Griffin, R. J., Herndon, S. C., Holloway, J. S., Holzinger, R., Jimenez, J. L., Junkermann, W., Kuster, W. C., Lewis, A. C., Meinardi, S., Millet, D. B., Onasch, T., Polidori, A., Quinn, P. K., Riemer, D. D., Roberts, J. M., Salcedo, D., Sive, B., Swanson, A. L., Talbot, R., Warneke, C., Weber, R. J., Weibring, P., Wennberg, P. O., Worsnop, D. R., Wittig, A. E., Zhang, R., Zheng, J., and Zheng, W.: Total observed organic carbon (TOOC) in the atmosphere: a synthesis of North American observations, Atmos. Chem. Phys., 8, 2007–2025, doi:10.5194/acp-8-2007-2008, 2008.

Judd, A. G., Hovland, M., Dimitrov, L. I., García Gil, S., and Jukes, V.: The geological methane budget at Continental Margins and its influence on climate change, Geofluids, 2, 109–126, doi:10.1046/j.1468-8123.2002.00027.x, 2002.

Jurado, E., Dachs, J., Duarte, C. M., and Simó, R.: Atmospheric deposition of organic and black carbon to the global oceans, Atmos. Environ., 42, 7931–7939, 2008.

Kähler, P., Bjornsen, P. K., Lochte, K., and Antia, A.: Dissolved organic matter and its utilization by bacteria during spring in the Southern Ocean, Deep-Sea Res. Pt. II, 44, 341–353, doi:10.1016/S0967-0645(96)00071-9, 1997.

Kuzma, J., Nemecek-Marshall, M., Pollock, W. H., and Fall, R.: Bacteria produce the volatile hydrocarbon isoprene, Curr. Microbiol., 30, 97–103, 1995.

Lancelot, C., Mathot, S., Veth, C., and Baar, H.: Factors controlling phytoplankton ice-edge blooms in the marginal ice-zone of the northwestern Weddell Sea during sea ice retreat 1988: Field observations and mathematical modeling, Polar Biol., 13, 377–387, doi:10.1007/BF01681979, 1993.

Laturnus, F.: Marine macroalgae in polar regions as natural sources for volatile organohalogens, Environ. Sci. Pollut. Res., 8, 103–108, doi:10.1007/BF02987302, 2001.

Laturnus, F., Giese, B., Wiencke, C., and Adams, F. C.: Low-molecular-weight organoiodine and organobromine compounds released by polar macroalgae – The influence of abiotic factors, Fresenius J. Anal. Chem., 368, 297–302, doi:10.1007/s002160000491, 2000.

Lechtenfeld, O. J., Koch, B. P., Gašparović, B., Frka, S., Witt, M., and Kattner, G.: The influence of salinity on the molecular and optical properties of surface microlayers in a karstic estuary, Mar. Chem., 150, 23–58, 2013.

Liss, P. S. and Duce, R. A. (Eds.).: The sea surface and global change, Cambridge University Press, 2005.

Llabrés, M. and Agustí, S.: Effects of ultraviolet radiation on growth, cell death and the standing stock of Antarctic phytoplankton, Aquat. Microb. Ecol., 59, 151–160, doi:10.3354/ame01392, 2010.

Madronich, S., McKenzie, R. L., Björn, L. O., and Caldwell, M. M.: Changes in biologically active ultraviolet radiation reaching the Earth's surface, J. Photochem. Photobiol. B, 46, 5–19, 1998.

Mayzaud, P., Boutoute, M., Gasparini, S., Mousseau, L., and Lefevre. D.: Respiration in Marine Zooplankton: The Other Side of the Coin: CO_2 Production, Limnol. Oceanogr., 50, 291–298, 2005.

Møller, E. F.: Sloppy feeding in marine copepods: prey-size-dependent production of dissolved organic carbon, J. Plankton Res., 27, 27–35, 2005.

Møller, E. F.: Production of dissolved organic carbon by sloppy feeding in the copepods Acartia tonsa, Centropages typicus, and Temora longicornis, Limnol. Oceanogr., 52, 79–84, 2007.

Mura, M. P., Satta, M. P., and Agustí, S.: Water-mass influences on summer Antarctic phytoplankton biomass and community structure, Polar Biol., 15, 15–20, 1995.

Murray, A. W. A.: Comparison of geostatistical and random sample survey analyses of Antarctic krill acoustic data, ICES J. Mar. Sci., 53, 415–421, doi:10.1006/jmsc.1996.0058, 1996.

Nightingale, P. D., Malin, G., Law, C. S., Watson, A. J., Liss, P. S., Liddicoat, M. I., Boutin, J., and Upstill-Goddard, R. C.: In situ evaluation of air-sea gas exchange parameterizations using novel conservative and volatile tracers, Global Biogeochem. Cy., 14, 373–387, doi:10.1029/1999GB900091, 2000.

Parsons, T. R., Maita, Y., and Lalli, C. M.: A manual of chemical and biological methods for seawater analysis, Pergamon press, Oxford, 1984.

Priddle, J., Brandini, F., Lipski, M., and Thorley, M. R.: Pattern and variability of phytoplankton biomass in the Antarctic Peninsula region: an assessment of the BIOMASS cruises, in: Southern Ocean ecology: the BIOMASS perspective, edited by: Sayed, S. Z., Cambridge University Press, Cambridge, 49–62, 1994.

Ruiz-Halpern, S., Sejr, M. K., Duarte, C. M., Krause-Jensen, D., Dalsgaard, T., Dachs, J., and Rysgaardd, S.: Air–water exchange and vertical profiles of organic carbon in a subarctic fjord, Limnol. Oceanogr., 55, 1733–1740, 2010.

Ruiz-Halpern, S., Duarte, C. M., Tovar-Sanchez, A., Pastor, M., Horstkotte, B., Lasternas, S., and Agustí, S.: Antarctic krill as a major source of dissolved organic carbon to the Antarctic ecosystem, Limnol. Oceangr., 56, 521–528, doi:10.4319/lo.2011.56.2.0521, 2011.

Sabine, C. L., Feely, R. A., Gruber, N., Key, R. M., Lee, K., Bullister, J. L., Wanninkhof, R., Wong, C. S., Wallace, D. W. R., Tilbrook, B., Millero, F. J., Peng, T. H., Kzyr, A., Ono, T., and Rioas, A. I.: The oceanic sink for anthropogenic CO_2, Science, 305, 367–371, doi:10.1126/science.1097403, 2004.

Schwarzenbach, R. P., Gschwend, P. M., and Imboden, D. M.: Environmental Organic Chemistry, 2nd Edn., Willey-Interscience, 2003.

Siedler, G., Church, J., Gould, J., and Griffies, S.: Ocean circulation and climate: observing and modelling the global ocean, Academic Press, San Diego, USA, 2001.

Sinha, V., Williams, J., Meyerhöfer, M., Riebesell, U., Paulino, A. I., and Larsen, A.: Air-sea fluxes of methanol, acetone, acetaldehyde, isoprene and DMS from a Norwegian fjord following a phytoplankton bloom in a mesocosm experiment, Atmos. Chem. Phys., 7, 739–755, doi:10.5194/acp-7-739-2007, 2007.

Smith Jr., K. L., Robison, B. H., Helly, J. J., Kaufmann, R. S., Ruhl, H. A., Shaw, T. J., Twining, B. S., and Vernet, M.: Free-drifting icebergs: Hot spots of chemical and biological enrichment in the Weddell Sea, Science, 317, 478–482, doi:10.1126/science.1142834, 2007.

Solomon, S., Qin, D., Manning, M., Chen, Z., Marquis, M., Averyt, K. B., Tignor, M., and Miller, H. L.: Climate change 2007-the physical science basis: Contribution of working group I to the fourth assessment report of the IPCC, Cambridge University Press, Cambridge, UK, 2007.

Spyres, G., Nimmo, M., Worsfold, P. J., Achterberg, E. P., and Miller, A. E. J.: Determination of dissolved organic carbon in seawater using high temperature catalytic oxidation techniques, TrAC-Trend. Anal. Chem., 19, 498–506, 2000.

Staudinger, J. and Roberts, P. V.: A critical compilation of Henry's law constant temperature dependence relations for organic compounds in dilute aqueous solutions, Chemosphere, 44, 561–576, 2001.

Takahashi, T., Feely, R. A., Weiss, R. F., Wanninkhof, R. H., Chipman, D. W., Sutherland, S. C., and Takahashi, T. T.: Global air-sea flux of CO_2: An estimate based on measurements of sea–air $p$$CO_2$ difference, P. Natl. Acad. Sci. USA, 94, 8292–8299, 1997.

Takahashi, T., Sutherland, S. C., Wanninkhof, R., Sweeney, C., Feely, R. A., Chipman, D. W., Hales, B., Friederich, G., Chavez, F., Sabine, C., Watson, A., Bakker, D. C. E., Schuster, U., Metzl, N., Yoshikawa-Inoue, H., Ishii, M., Midorikawa, T., Nojiri, Y., Körtzinger, A., Steinhoff, T., Hoppema, M., Olafsson, J., Arnarson, T. S., Tilbrook, B., Johannessen, T., Olsen, A., Bellerby, R., Wong, C. S., Delille, B., Bates, N. R., and de Baar. H. J. W.: Climatological mean and decadal change in surface ocean $p$$CO_2$, and net sea-air CO_2 flux over the global oceans, Deep-Sea Res. Pt. II, 56, 554–577, doi:10.1016/j.dsr2.2008.12.009, 2009.

Villaverde, S. and Fernandez-Polanco, F.: Spatial distribution of respiratory activity in Pseudomonas putida 54G biofilms degrading volatile organic compounds (VOC), Appl. Microbiol. Biotechnol., 51, 382–387, doi:10.1007/s002530051406, 1999.

Weiss, R. F.: Carbon dioxide in water and seawater: the solubility of a non-ideal gas, Mar. Chem., 2, 203–215, doi:10.1016/0304-4203(74)90015-2, 1974.

Yang, M., Nightingale, D., Beale, R., Liss, P., Blomquist, B., and Fairall, F.: Atmospheric deposition of methanol over the Atlantic Ocean, P. Natl. Acad. Sci. USA, 110, 20034–20039, doi:10.1073/pnas.1317840110, 2013

Young, I. R., Zieger, S., and Babanin, A. V.: Global trends in wind speed and wave height, Science, 332, 451–455, doi:10.1126/science.1197219, 2011

Zepp, R. G., Callaghan, T. V., and Erickson, D. J.: Effects of enhanced solar ultraviolet radiation on biogeochemical cycles, J. Photochem. Photobiol. B, 46, 69–82, doi:10.1016/S1011-1344(98)00186-9, 1998.

Zhou, M. and Dorland, R. D.: Aggregation and vertical migration behavior of *Euphausia superba*, Deep-Sea Res. Pt. II, 51, 2119–2137, doi:10.1016/j.dsr2.2004.07.009, 2004.